ELSEVIER

Biophysical Chemistry 78 (1999) 1–20

Biophysical Chemistry

Implicit solvent models

Benoît Roux[a,*], Thomas Simonson[b]

[a] *Départements de physique et de chimie, Université de Montréal, C.P. 6128, succursale, Centre-Ville, Montréal, QC, Canada H3C 3J7*

[b] *Laboratoire de Biologie Structurale (C.N.R.S.), I.G.B.M.C., 1 rue Laurent Fries, 67404 Strasbourg-Illkirch, France*

Received 19 November 1998; accepted 23 November 1998

Abstract

Implicit solvent models for biomolecular simulations are reviewed and their underlying statistical mechanical basis is discussed. The fundamental quantity that implicit models seek to approximate is the solute potential of mean force, which determines the statistical weight of solute conformations, and which is obtained by averaging over the solvent degrees of freedom. It is possible to express the total free energy as the reversible work performed in two successive steps. First, the solute is inserted in the solvent with zero atomic partial charges; second, the atomic partial charges of the solute are switched from zero to their full values. Consequently, the total solvation free energy corresponds to a sum of non-polar and electrostatic contributions. These two contributions are often approximated by simple geometrical models (such as solvent exposed area models) and by macroscopic continuum electrostatics, respectively. One powerful route is to approximate the average solvent density distribution around the solute, i.e. the solute–solvent density correlation functions, as in statistical mechanical integral equations. Recent progress with semi-analytical approximations makes continuum electrostatics treatments very efficient. Still more efficient are fully empirical, knowledge-based models, whose relation to explicit solvent treatments is not fully resolved, however. Continuum models that treat both solute and solvent as dielectric continua are also discussed, and the relation between the solute fluctuations and its macroscopic dielectric constant(s) clarified.

1. Introduction

Computer simulations in which a large number of solvent molecules are treated explicitly represent one of the most detailed approaches to study the influence of solvation on complex biomolecules [1]. However, a significant computational cost is associated with the large number of solvent molecules required to model a bulk solution. In practical situations, a large fraction of the time is spent calculating a detailed trajectory of the solvent molecules, even though it is primarily the solute behavior that is of interest. Furthermore, despite their cost, computer simulations with explicit solvent molecules are not exempt from approximations. For example, difficulties arise in thermodynamic perturbation free energy

* Corresponding author. Fax: +1 514 343 7586.

0301-4622/99/$ - see front matter
PII: S0301-4622(98)00226-9

calculations involving charged species when long range electrostatic interactions are truncated or summed over an infinite periodic array using Ewald techniques [2].

Partly due to these difficulties, it is desirable to develop different approaches in which the influence of the solvent is incorporated implicitly. Approximate schemes treating the solvent implicitly can provide useful quantitative estimates and remain computationally inexpensive. Such approaches avoid the statistical errors associated with averages extracted from simulations with a large number of solvent molecules. In addition, implicit solvent models can play an important role as conceptual tools for analyzing the results of simulations generated with explicit solvent molecules. A statistical mechanical formulation of implicit solvent is helpful to better understand the nature of solvation phenomena in general.

The goal of this article is to provide an overview of implicit solvent models commonly used in biomolecular simulations. A number of questions concerning the formulation and the development of implicit solvent models are addressed. The article begins with a rigorous formulation of implicit solvent from statistical mechanics. The potential of mean force (PMF) is introduced. A decomposition in terms of non-polar and electrostatic contributions is described. Approximations such as integral equations, scaled particle theory, and classical continuum electrostatics are discussed. Solvent boundary potentials for implicit/explicit mixed schemes are briefly reviewed. Continuum models of both solute and solvent are also described. Lastly, miscellaneous approximations of implicit solvation are discussed. The paper ends with a short summary.

2. Rigorous formulation of implicit solvent models

First and foremost, it is important to clarify the significance of implicit solvent models from first principles. To this effect, we consider a molecular solute immersed in a solvent in contact with a heat bath at temperature T. It is expected that the system is fluctuating over a large number of configurations. The statistical properties of the system are best characterized in terms of a probability function $P(\mathbf{X},\mathbf{Y})$ [3],

$$P(\mathbf{X},\mathbf{Y}) = \frac{\mathrm{e}^{-U(\mathbf{X},\mathbf{Y})/k_{\mathrm{B}}T}}{\int \mathrm{d}\mathbf{X}\,\mathrm{d}\mathbf{Y}\,\mathrm{e}^{-U(\mathbf{X},\mathbf{Y})/k_{\mathrm{B}}T}} \tag{1}$$

where the complete configuration of the solute 'u' and the solvent 'v' atoms are specified by the coordinates $\mathbf{X} \equiv \{\mathbf{x}_1, \mathbf{x}_2, \ldots\}$ and $\mathbf{Y} \equiv \{\mathbf{y}_1, \mathbf{y}_2, \ldots\}$, respectively. For the sake of simplicity, we will assume that the total potential energy can be decomposed as

$$U(\mathbf{X},\mathbf{Y}) = U_{\mathrm{u}}(\mathbf{X}) + U_{\mathrm{vv}}(\mathbf{Y}) + U_{\mathrm{uv}}(\mathbf{X},\mathbf{Y}) \tag{2}$$

where $U_{\mathrm{u}}(\mathbf{X})$ is the intramolecular solute potential, $U_{\mathrm{vv}}(\mathbf{Y})$ is the solvent–solvent potential, and $U_{\mathrm{uv}}(\mathbf{X},\mathbf{Y})$ is the solute–solvent potential.

All the properties of a molecular system are fundamentally related to averages weighted by the probability function $P(\mathbf{X},\mathbf{Y})$. For example, for any quantity $Q(\mathbf{X})$ depending on the solute configuration

$$\langle Q \rangle = \int \mathrm{d}\mathbf{X}\,\mathrm{d}\mathbf{Y}\,Q(\mathbf{X})\,P(\mathbf{X},\mathbf{Y}). \tag{3}$$

An important question is whether one can rigorously express such an average without referring explicitly to the solvent degrees of freedom $\mathbf{Y}$. In other words: is it possible to 'get rid' of the solvent in the mathematical description of the molecular system and still obtain correct properties? The answer to the question is yes. A reduced probability distribution $\bar{P}(\mathbf{X})$ that depends only on the solute configuration can be defined as

$$\bar{P}(\mathbf{X}) = \int \mathrm{d}\mathbf{Y}\,P(\mathbf{X},\mathbf{Y}). \tag{4}$$

The reduced probability distribution does not depend explicitly on the solvent degrees of freedom, although the average influence of the solvent is taken into account. This operation is commonly described by saying that the solvent coordinates have been 'integrated out'. In a system character-

ized by the canonical ensemble at temperature T, the reduced probability has the form

$$\bar{P}(\mathbf{X}) = \frac{\int d\mathbf{Y}\, e^{-[U_u(\mathbf{X})+U_{vv}(\mathbf{Y})+U_{uv}(\mathbf{X},\mathbf{Y})]/k_B T}}{\int d\mathbf{X}\, d\mathbf{Y}\, e^{-[U_u(\mathbf{X})+U_{vv}(\mathbf{Y})+U_{uv}(\mathbf{X},\mathbf{Y})]/k_B T}} = \frac{e^{-W(\mathbf{X})/k_B T}}{\int d\mathbf{X}\, e^{-W(\mathbf{X})/k_B T}}. \quad (5)$$

The function $W(\mathbf{X})$ is called the 'potential of mean force' (PMF). The concept of the PMF was first introduced by Kirkwood to describe the average structure of liquids [4]. It is easy to show that for cartesian coordinates, the gradient of $W(\mathbf{X})$ is simply related to the average force

$$\frac{\partial W(\mathbf{X})}{\partial \mathbf{x}_i} = \left\langle \frac{\partial U}{\partial \mathbf{x}_i} \right\rangle_{(\mathbf{X})} = -\langle \mathbf{F}_{\mathbf{x}_i} \rangle_{(\mathbf{X})} \quad (6)$$

where $\boldsymbol{x}_i$ is the position of the ith solute atom and the symbol $\langle \cdots \rangle_{(\mathbf{X})}$ represents an average over all coordinates of the solvent, for a solute in the fixed configuration specified by $\mathbf{X}$. The PMF is the reversible work done by the average force. In particular, it should be emphasized that the PMF is not equal to an average potential energy, that is,

$$W(\mathbf{X}) \neq \langle U \rangle_{(\mathbf{X})}. \quad (7)$$

All solvent effects are included in $W(\mathbf{X})$ and, consequently, in the reduced distribution function $\bar{P}(\mathbf{X})$. For example, if a quantity $Q(\mathbf{X})$ depends only on the solute configuration, it is possible to express its average rigorously,

$$\langle Q \rangle = \int d\mathbf{X}\; Q(\mathbf{X})\; \bar{P}(\mathbf{X}) = \int d\mathbf{X}\, d\mathbf{Y}\; Q(\mathbf{X})\; P(\mathbf{X},\mathbf{Y}) \quad (8)$$

recovering the exact expression of Eq. (3) for the average of Q. Therefore, there exists an effective potential $W(\mathbf{X})$, making no explicit reference to the solvent degrees of freedom, such that no information about the influence of solvent on equilibrium properties is lost.

3. The potential of mean force $W(\mathbf{X})$

3.1. Relative and absolute values: reversible work

As long as the normalization condition given by Eq. (5) is satisfied, an arbitrary offset constant may be added to $W(\mathbf{X})$ without affecting averages in Eq. (8). The absolute value of the PMF is thus unimportant. For convenience, it is possible to choose the value of the free energy $W(\mathbf{X})$ relative to a reference system in which the solute–solvent interactions are absent. The free energy $W(\mathbf{X})$ may be expressed as

$$e^{-W(\mathbf{X})/k_B T} = \frac{\int d\mathbf{Y}\, e^{-[U_u(\mathbf{X})+U_{vv}(\mathbf{Y})+U_{uv}(\mathbf{X},\mathbf{Y})]/k_B T}}{\int d\mathbf{Y}\, e^{-U_{vv}(\mathbf{Y})/k_B T}}. \quad (9)$$

It is customary to write $W(\mathbf{X}) = U_u(\mathbf{X}) + \Delta W(\mathbf{X})$, where $U_u(\mathbf{X})$ is the intramolecular solute potential and $\Delta W(\mathbf{X})$ is the solvent-induced influence.

Introducing the thermodynamic solute–solvent coupling parameter λ, we write the potential energy as,

$$U(\mathbf{X},\mathbf{Y};\lambda) = U_u(\mathbf{X}) + U_{vv}(\mathrm{Y}) + U_{uv}(\mathbf{X},\mathbf{Y};\lambda) \quad (10)$$

constructed such that $\lambda = 0$ corresponds to a non-interacting reference system with $U_{uv}(\mathbf{X},\mathbf{Y};0) = 0$, and $\lambda = 1$ corresponds to the fully interacting system. As long as the end-points are respected, any form of thermodynamic coupling is correct. We have

$$\Delta W(\mathbf{X}) = \int_0^1 d\lambda \left\langle \frac{\partial U_{uv}}{\partial \lambda} \right\rangle_{(\mathbf{X},\lambda)} \quad (11)$$

where the symbol $\langle \cdots \rangle_{(\mathbf{X},\lambda)}$ represents an average over all coordinates of the solvent, for a solute in the fixed configuration specified by $\mathbf{X}$ with thermodynamic coupling λ. It is also possible to ex-

press relative values of the PMF between different solute configurations $\mathbf{X}_1$ and $\mathbf{X}_2$ using Eq. (6) and the reversible work theorem [4]

$$\Delta W(\mathbf{X}_2) = \Delta W(\mathbf{X}_1) + \int_{\mathbf{X}_1}^{\mathbf{X}_2} \mathrm{d}\mathbf{X} \cdot \frac{\partial \Delta W(\mathbf{X})}{\partial \mathbf{X}} = W(\mathbf{X}_1) + \int_{\mathbf{X}_1}^{\mathbf{X}_2} \sum_i \mathrm{d}\mathbf{x}_i \cdot \left\langle \frac{\partial U_{\mathrm{uv}}}{\partial \mathbf{x}_i} \right\rangle_{(\mathbf{X},\lambda)} . \tag{12}$$

It may be noted that $\langle \partial U_{\mathrm{uv}}/\partial\lambda \rangle_{(\mathbf{X},\lambda)}$ in Eq. (11) plays the role of a generalized thermodynamic force similar to that of $\langle \partial U/\partial \mathbf{x}_i \rangle_{(\mathbf{X})}$ in Eq. (12).

3.2. Thermodynamics and state dependence

The PMF plays the role of an effective free energy potential. It is state-dependent, i.e. it depends on the temperature T and the pressure p. Thus, one should formally write $W(\mathbf{X};T,p)$. For a fixed solute configuration $\mathbf{X}$, the PMF can be decomposed thermodynamically as

$$\Delta W(\mathbf{X}) = \Delta E(\mathbf{X}) - T\Delta S(\mathbf{X}) \tag{13}$$

where $\Delta S(\mathbf{X}) = -\partial \Delta W(\mathbf{X})/\partial T$ is the solvent entropy for the solute in the fixed configuration $\mathbf{X}$. All quantities are excesses with respect to the reference system in which the solute–solvent interactions are absent. The excess chemical potential $\Delta\mu$ of the solute (i.e. the solvation free energy) is

$$\mathrm{e}^{-\Delta\mu/k_{\mathrm{B}}T} = \frac{\int \mathrm{d}\mathbf{X}\, \mathrm{e}^{-[U_{\mathrm{u}}(\mathbf{X}) + \Delta W(\mathbf{X})]/k_{\mathrm{B}}T}}{\int \mathrm{d}\mathbf{X}\, \mathrm{e}^{-U_{\mathrm{u}}(\mathbf{X})/k_{\mathrm{B}}T}} = \langle \mathrm{e}^{-\Delta W(\mathbf{X})/k_{\mathrm{B}}T} \rangle_{(U_{\mathrm{u}})}. \tag{14}$$

The last expression has been written in the well-known free energy perturbation form [5]. The integration is over all degrees of freedom of the solute, and the subscript U_{u} indicates that an average is performed corresponding to the Boltzmann weight $\exp[-U_{\mathrm{u}}(\mathbf{X})/k_{\mathrm{B}}T]$, U_{u} being the intramolecular potential of the isolated solute. To obtain a closed-form expression for the chemical potential, it is sometimes useful to evaluate the configurational integrals in Eq. (14) with a quasi-harmonic approximation [6].

A thermodynamic decomposition of the solute excess chemical potential is possible using temperature derivatives, i.e. $\Delta\mu = \Delta e - T\Delta s$, with $\Delta s = -\partial\Delta\mu/\partial T$, giving

$$\Delta s = \left[\frac{-\Delta\mu}{T} + \frac{\langle W \rangle_{(W)} - \langle U_{\mathrm{u}} \rangle_{(U_{\mathrm{u}})}}{T} \right] - \left\langle \frac{\partial \Delta W}{\partial T} \right\rangle_{(W)} \tag{15}$$

The first term can be thought of as the excess configurational entropy of the solute. The last term corresponds to the solvent entropy averaged over all solute configurations $\mathbf{X}$, weighted by the Boltzmann factor $\exp[-W(\mathbf{X})/k_{\mathrm{B}}T]$. For example, only the first term would contribute to Δs if the effect of solvent was only to reduce the configurational space accessible to the solute. Such a separation into a solute configurational entropy and a solvent entropy is not straightforward in the case of simulations with explicit solvent.

Similarly, the specific molar volume of the solute can also be obtained if the implicit solvent model takes the influence of pressure into account,

$$\Delta\nu_{\mathrm{mol}} = \frac{\partial\Delta\mu}{\partial p} = \left\langle \frac{\partial \Delta W}{\partial p} \right\rangle_{(W)} \tag{16}$$

The factor $\partial\Delta W/\partial p$ can be thought of as a configuration-dependent molar volume of the solute. The specific molar volume $\Delta\nu_{\mathrm{mol}}$ is an average over all the accessible configurations $\mathbf{X}$ of the solute.

3.3. Ligand–protein association constant

A formulation of implicit solvent is useful to describe ligand–protein association. Let $\mathbf{X}_{\mathrm{L}}$ be the degrees of freedom of the ligand, and $\mathbf{X}_{\mathrm{P}}$ be the degrees of freedom of the protein. The PMF for the ligand–protein complex is $W_{\mathrm{LP}}(\mathbf{X}_{\mathrm{L}},\mathbf{X}_{\mathrm{P}})$; the PMFs for the isolated ligand and protein are

$W_L(\mathbf{X}_L)$ and $W_P(\mathbf{X}_P)$, respectively. The association constant is [7]

$$K = \frac{\int_{\text{bound}} d\mathbf{X}_L d\mathbf{X}_P \; e^{-W_{LP}(\mathbf{X}_L,\mathbf{X}_P)/k_B T}}{\int d\mathbf{X}_L \; \delta(\mathbf{x}_{cm}) e^{-W_L(\mathbf{X}_L)/k_B T} \int d\mathbf{X}_P \; e^{-W_P(\mathbf{X}_P)/k_B T}} \tag{17}$$

The integral in the numerator is taken over all configurations of the ligand and the protein such that the complex is in the bound state. The final constant K has dimensions of volume, which yields a dimensionless factor in the probability of occupancy, $K[C]/(1+K[C])$, where $[C]$ is the concentration of ligands. The delta function in the denominator insures that global translation of the ligand center of mass is removed in the unbound reference state. For the sake of simplicity, it is often advantageous to remove also the global translation and rotation of the complex and of the isolated protein (in the numerator and the denominator, respectively) since they do not contribute to the binding constant.

3.4. Time-dependent properties

It is attractive to use the PMF obtained from an implicit solvent model to describe the dynamical, time-dependent properties of the solute. For dense liquid systems, the classical Langevin equation for the atom i.

$$m_i \ddot{\mathbf{x}}_i = -\frac{\partial W(\mathbf{X})}{\partial \mathbf{x}_i} - \sum_j \gamma_{ij} \dot{\mathbf{x}}_j(t) + f_i(t) \tag{18}$$

can provide a reasonable approximation of the solute dynamics [3]. In the Langevin equation, the force $f_i(t)$ is a random Gaussian variable, and integration of Eq. (18) leads to stochastic trajectories. The influence of the random and dissipative forces determine the time-scale of the dynamics, while the equilibrium time-independent properties are controlled by the PMF. If one is exclusively interested in the latter, the value of the friction coefficients γ_{ij} is only a matter of convenience, i.e. the Boltzmann distribution $\bar{P}(\mathbf{X}) \propto \exp[-W(\mathbf{X})/k_B T]$ of Eq. (4) follows directly, regardless of the magnitude of the friction coefficient γ_{ij}, as long as the random force satisfies the second fluctuation–dissipation theorem: $\langle f_i(t) f_j(0) \rangle = 2 k_B T \gamma_{ij} \delta(t)$ [3]. Performing a Langevin dynamics with the gas phase potential $U_u(\mathbf{X})$ does not incorporate any solvation effects into the equilibrium properties. Because they are computationally inexpensive, Langevin dynamics can be advantageous to investigate the time-dependent properties of some systems. This approach has been used to examine the conformational fluctuations of small polypeptides in water [8].

The classical Langevin Eq. (18) with constant friction coefficients is a somewhat crude approximation that ignores the time-dependent response of the solute surroundings (the random force is completely uncorrelated at all times). More sophisticated stochastic models, which reproduce the detailed dynamical behavior of a true microscopic system more realistically, can be constructed by using a generalized Langevin equation with memory [9,10],

$$m_i \ddot{\mathbf{x}}_i = -\frac{\partial W(\mathbf{X})}{\partial \mathbf{x}_i} - \int_0^t dt' \sum_j \gamma_{ij}(t-t') \dot{\mathbf{x}}_j(t') + f_i(t) \tag{19}$$

In particular, one may be interested in incorporating the frequency dependence of the dielectric response of the solvent into a reaction field description [12]. In this case, the time-independent properties will be in accord with the Boltzmann distribution if, and only if, the random force and the time-dependent friction satisfy the generalized second fluctuation–dissipation theorem [11],

$$\langle f_i(t) f_j(t') \rangle = k_B T \gamma_{ij}(t-t') \tag{20}$$

Thus, in constructing a generalized Langevin equation with memory it is essential that the random force be consistent with the time-dependent friction. Using a time-dependent memory function with uncorrelated random forces [12]

leads to a non-equilibrium stationary state which differs from the correct thermal ensemble.

3.5. Average solvent density and integral equations

The calculation of the reversible work in Eq. (11) involves configurational averages which can in principle be obtained from computer simulations. For example, such averages can be expressed as

$$\left\langle \frac{\partial u}{\partial \lambda} \right\rangle_{(\mathbf{X},\lambda)} = \frac{1}{N_{\mathrm{conf}}} \sum_{n=1}^{N_{\mathrm{conf}}} \frac{\partial U(\mathbf{X},\mathbf{Y}_n;\lambda)}{\partial \lambda} \tag{21}$$

Alternatively, assuming that the solute–solvent interaction can be written as a pairwise sum of contributions over individual solvent molecules m in the configuration $\mathbf{y}$ (including positional, orientational and internal degrees of freedom), the average can be written as an integral,

$$\begin{aligned} \left\langle \frac{\partial U}{\partial \lambda} \right\rangle_{(\mathbf{X},\lambda)} &= \left\langle \frac{\partial}{\partial \lambda} \sum_m u_{\mathrm{uv}}(\mathbf{X},\mathbf{y}_m;\lambda) \right\rangle_{(\mathbf{X},\lambda)} \\ &= \int \mathrm{d}\mathbf{y} \left\langle \sum_m \delta(\mathbf{y}-\mathbf{y}_m) \right\rangle_{(\mathbf{X},\lambda)} \frac{\partial u_{\mathrm{uv}}(\mathbf{X},\mathbf{y};\lambda)}{\partial \lambda} \\ &= \int \mathrm{d}\mathbf{y} \, \langle \rho(\mathbf{y}) \rangle_{(\mathbf{X},\lambda)} \frac{\partial u_{\mathrm{uv}}(\mathbf{X},\mathbf{y};\lambda)}{\partial \lambda}, \end{aligned} \tag{22}$$

where $\langle \rho(\mathbf{y}) \rangle_{(\mathbf{X},\lambda)}$ is the average solvent density for finding a molecule in configuration $\mathbf{y}$ (including position, orientation and internal degrees of freedom) around the solute in the fixed configuration $\mathbf{X}$. Eqs. (21) and (22) are equivalent if the exact solvent density is used. Finding suitable approximations for the average solvent density, as in liquid state integral equation theories [3,13,14], is a powerful route for developing implicit solvent models. For this reason, a formulation of the PMF based on Eq. (22) is particularly useful.

Liquid state integral equations are sophisticated statistical mechanical theories [3,13,14] which can provide a rigorous framework for calculating the average solvent density around a complex solute of arbitrary shape. Average solvent structures caused by the granularity, packing, hydrogen bonding and other associative forces, as well as long-range dielectric shielding and ionic screening, are all examples of important effects that can be incorporated using integral equations [13,14]. A complete review of integral equations would be beyond the scope of this article, therefore we will only provide a brief overview of this vast and important field.

One of the simplest theories to describe the average solvent density $\langle \rho(r) \rangle$ in the neighborhood of a spherical monoatomic solute immersed in a simple liquid is the hypernetted chain (HNC) equation [13].

$$\langle \rho(r) \rangle = \bar{\rho} \mathrm{e}^{-u(r)/k_{\mathrm{B}}T + c * \Delta\rho(r)}, \tag{23}$$

where $\bar{\rho}$ is the bulk density, $u(r)$ is the perturbing potential acting on the solvent due to the solute, $c(r)$ is the direct correlation function of the unperturbed uniform bulk fluid, the symbol $*$ represents a three-dimensional spatial convolution, and $\Delta\rho(r) = \rho(r) - \bar{\rho}$ is the deviation from the bulk density at a distance r from the solute. More sophisticated integral equation theories with a similar basic structure have also been proposed. In particular, the reference HNC equation (R-HNC) [15], is an advanced integral equation theory able to provide detailed information about the positional and orientational pair distribution functions of the solvent around a solute. Theories based on site-site radial distribution functions such as the reference interaction site model (RISM) equation are computationally simpler [14,16]. Such theories are based upon the Chandler–Andersen (or site–site Ornstein–Zernike) equation [16].

$$\mathbf{h}(r) = \boldsymbol{\omega} * \mathbf{c} * \boldsymbol{\omega}(r) + \boldsymbol{\omega} * \mathbf{c} * \rho \mathbf{h}(r) \tag{24}$$

where $\mathbf{h}(r)$ is the site–site pair correlation function, $\mathbf{c}(r)$ is the site–site direct correlation function, and $\boldsymbol{\omega}$ is the intra-molecular correlation matrix. The RISM theory has been used in combination with a site–site HNC closure to describe polar systems [17]

$$h_{ij}(r) = \mathrm{e}^{-u_{ij}(r)/k_{\mathrm{B}}T + \phi_{ij}(r) + h_{ij}(r) - c_{ij}(r)} - 1 \tag{25}$$

where $\phi_{ij}(r) = -q_i q_j/(k_B T r)$ is the long range site–site Coulomb interaction, and $u_{ij}(r)$ is the remaining short range part of the potential. The RISM theory has been used to study the hydration of mono-atomic solutes [18,19], small peptides [20–22], and many other organic solutes [23,24]. A related approach has been used to examine hydrophobic solvation [25]. However, the theory is not appropriate for large molecular solutes, since completely buried atoms of the solute are only partially shielded from the solvent in RISM (i.e. the solvent density around an atom located in the center of a structure is not zero). Furthermore, the dielectric constant of the pure liquid is not described satisfactorily. There have been several efforts to correct the deficiencies of the theory. For example, a reformulated dielectrically consistent RISM equation was developed to model finite-concentration salt solutions [26].

Since RISM theories are based on a reduction to site–site solute–solvent radially symmetric distribution functions, there is a loss of information about the three-dimensional spatial organization of the solvent density around a non-spherical molecular solute. Recently, it has been possible to formulate and solve integral equations able to take into account the full distribution of the solvent around solutes of irregular shape in three dimensions [27–31]. The 3d-HNC integral equation describing the density of a simple Lennard–Jones solvent around non-polar solutes of arbitrary shape were solved numerically on a three-dimensional grid. The spatial convolutions were calculated using fast Fourier transforms in three-dimensions. Extensions of RISM-like theories for three-dimensional space (3d-RISM) have been proposed and solved numerically [30,31].

Other approximations are also currently being explored. An extension to the mean-spherical-approximation integral equation in three dimensions (3d-MSA), describing the distribution function of a liquid of spherical molecules with an embedded dipole around a polar solute was formulated and solved numerically [29]. Using this theory, it was possible to demonstrate that the Poisson equation with a spatially-dependent dielectric constant E(**r**), such as used in macroscopic continuum solvation models (see Eq. (43) below), is obtained if the correlations in the liquid are short-ranged [29]. An integral equation describing the structure of water molecules in terms of sticky interaction points has been developed [32,33]. A theory based on an expansion in terms of two- and three-body correlation functions has been proposed to describe the hydration structure around nucleic acids [34] and proteins [35]. In summary, integral equations and theories based on distribution functions represent a powerful framework for developing new approaches to describe the solvation of biomolecules.

4. Free energy decomposition

Intermolecular forces are dominated by short-range harsh repulsive interactions, arising from Pauli's exclusion principle, and long-range electrostatic interactions, arising from the non-uniform charge distribution. It is convenient to express the potential energy $U_{uv}(\mathbf{X},\mathbf{Y})$ as a sum of non-polar and electrostatic contributions,

$$U_{uv}(\mathbf{X},\mathbf{Y}) = U_{uv}^{(np)}(\mathbf{X},\mathbf{Y}) + U_{uv}^{(elec)}(\mathbf{X},\mathbf{Y}). \quad (26)$$

Such a representation of the microscopic non-bonded interactions is commonly used in most force fields for computer simulations of biomolecules (e.g. AMBER [36], CHARMM [37], OPLS [38]).

The separation of the non-bonded interactions is useful for decomposing the reversible work that defines the function $W(\mathbf{X})$. We express the total free energy as the reversible work corresponding to two successive steps. In a first step, the non-polar solute–solvent interactions are switched on in the absence of any solute–solvent electrostatic interactions; in a second step, the solute–solvent electrostatic interactions are switched on in the presence of the solute–solvent non-polar interactions. The solute is kept in a fixed configuration **X** throughout both processes, and the intramolecular potential energy does not vary during this process. By construction, the total PMF is

$$W(\mathbf{X}) = U_u(\mathbf{X}) + \Delta W^{(np)}(\mathbf{X}) + \Delta W^{(elec)}(\mathbf{X}) \quad (27)$$

where the non-polar solvation contribution is

$$e^{-\Delta W^{(np)}(\mathbf{X})/k_B T} = \frac{\int d\mathbf{Y}\, e^{-[U_{vv}(\mathbf{Y})+U_{uv}^{(np)}(\mathbf{X},\mathbf{Y})]/k_B T}}{\int d\mathbf{Y}\, e^{-U_{vv}(\mathbf{Y})/k_B T}} \tag{28}$$

and the electrostatic solvation contribution is

$$e^{-\Delta W^{(elec)}(\mathbf{X})/k_B T} = \frac{\int d\mathbf{Y}\, e^{-[U_{vv}(\mathbf{Y})+U_{uv}^{(np)}(\mathbf{X},\mathbf{Y})+U_{uv}^{(elec)}(\mathbf{X},\mathbf{Y})]/k_B T}}{\int d\mathbf{Y}\, e^{-[U_{vv}(\mathbf{Y})+U_{uv}^{(np)}(\mathbf{X},\mathbf{Y})]/k_B T}}. \tag{29}$$

Combining Eqs. (27)–(29) yields Eq. (9) directly. Because the non-polar contribution is associated with the harsh repulsive potential. $\Delta W^{(np)}(\mathbf{X})$ is usually referred to as the 'free energy of cavity formation': the quantity $\Delta W^{(elec)}(\mathbf{X})$ is called the 'charging free energy'.

Equivalently, we can express the free energy in terms of two thermodynamic integration coupling parameters, λ_1 and λ_2 [39]. The potential energy is written

$$U(\mathbf{X},\mathbf{Y}:\lambda_1,\lambda_2) = U_u(\mathbf{X}) + U_{vv}(\mathbf{Y}) + U_{uv}^{(np)}(\mathbf{X},\mathbf{Y}:\lambda_1) + U_{uv}^{(elec)}(\mathbf{X},\mathbf{Y}:\lambda_2). \tag{30}$$

where $\lambda_1 = \lambda_2 = 0$ corresponds to the non-interacting reference system, $\lambda_1 = 1 = \lambda_2 = 1$ corresponds to the fully interacting system, and $\lambda_1 = 1$ with $\lambda_2 = 0$ corresponds to an intermediate system with no solute–solvent electrostatic interactions. Each contribution can be expressed as the reversible work from a thermodynamic integration,

$$\Delta W^{(np)}(\mathbf{X}) = \int_0^1 d\lambda_1 \left\langle \frac{\partial U^{(np)}}{\partial \lambda_1} \right\rangle_{(\mathbf{X},\lambda_1,\lambda_2=0)} \tag{31}$$

and

$$\Delta W^{(elec)}(\mathbf{X}) = \int_0^1 d\lambda_2 \left\langle \frac{\partial U^{(elec)}}{\partial \lambda_2} \right\rangle_{(\mathbf{X},\lambda_1=1,\lambda_2)}. \tag{32}$$

The free energy decomposition in Eq. (27) is, of course, path-dependent [40,41]. The non-polar and electrostatic contributions to the free energy depend on the order in which these successive steps are performed. For example, it is necessary to first insert the non-polar cavity into the solvent before performing the electrostatic charging of the solute; the opposite yields diverging results. Nevertheless, the decomposition can be useful for understanding the different microscopic factors playing an important role in solvation. In particular, the non-polar and electrostatic free energy contributions can be related to various approximate continuum descriptions (see below).

4.1. Non-polar contribution

It is instructive to first examine the contribution of non-polar interactions to the PMF. For the sake of simplicity, let us consider a spherical particle in water. According to Eq. (31), the non-polar free energy contribution can be expressed as a radial integral,

$$\Delta W^{(np)} = \int_0^1 d\lambda_1 4\pi \int_0^\infty r^2 dr\, \langle \rho(r) \rangle_{(\lambda_1)} \frac{\partial u_{uv}^{(np)}(r;\lambda_1)}{\partial \lambda_1} \tag{33}$$

where $\langle \rho(r) \rangle_{(\lambda_1)}$ is the average density of the water oxygen around the spherical particle, and the water hydrogens are assumed to have no van der Waals interactions with the solute. By definition, $\lambda_2 = 0$ in this step, i.e. the solute has no partial charges. It is convenient to choose the thermodynamic coupling parameter λ_1 as a scaling factor applied to the radius of the solute particle. The derivative of the function $u_{uv}^{(np)}(r:\lambda_1)$ with respect to λ_1 decreases very abruptly as a function of distance from the center of the solute. In contrast, the density $\langle \rho(r) \rangle_{(\lambda_1)}$ vanishes inside the core of the solute. The product of the two functions is a sharply peaked function that is

non-vanishing mainly at the contact distance. This observation is exploited to obtain approximate forms of the non-polar contribution to the free energy solvation in 'scaled-particle theory' (SPT) [42–44] and 'solvent-exposed surface area' models [46]. Those approaches are described in the following. Nonetheless, it should be emphasized that neither SPT nor solvent-exposed surface models provide an ultimate representation of the non-polar contribution to the solvation free energy. Even today, elucidating the fundamental nature of hydrophobic solvation at short and long range remains a central problem in theoretical biophysics. In that regard, new approaches based on cavity-size distributions [47,48] and on free energy density functionals (Chandler and Weeks, unpublished) presently being developed appear promising.

4.1.1. Scaled particle theory

A simple approach was proposed by Reiss et al. [42], Stillinger [43], and Pierotti [44] to describe the free energy of inserting a non-polar repulsive sphere into a solvent. The approach is called 'scaled particle theory' (SPT) because it is based on arguments involving the scaling of the repulsive sphere radius. The reversible work $W(R)$ to produce a spherical cavity of radius R can be calculated exactly for a hard-sphere liquid of bulk density $\bar{\rho}$ as long as $2R \leq a$, the hard sphere diameter:

$$W(R) = -k_B T \ln\left(1 - \frac{4}{3}\pi R^3 \bar{\rho}\right). \quad (34)$$

For a non-polar solute in liquid water, a is assigned a value of 2.75 Å, corresponding to the distance of closest contact in the oxygen–oxygen radial distribution function of liquid water [43]. For a soft-sphere solute interacting with the solvent through $u(r) = \lambda A r^{-n}$, R is an equivalent hard-sphere radius which can be written $R = (3B/2\pi)^{1/3}$, where B is the second virial coefficient, $B = (2\pi/3)(\lambda A/k_B T)^{3/n}\Gamma((n-3)/3)$, and Γ is the Gamma function. Generalizations to van der Waals and associated liquids have been made by introducing experimental densities and virial coefficients. In the limit of a large cavity or solute particle, thermodynamic considerations [45] lead to

$$W(R) = \frac{4}{3}\pi R^3 p + 4\pi R^2 \gamma_v \left(1 - \frac{4\delta}{R}\right) + \ldots \quad (35)$$

where p is the isotropic pressure chosen according to experimental conditions, γ_v the surface tension of the solvent, and δ is a molecular length scale. The remaining terms are assumed to be negligible. In effect, this expression implies that the microscopic surface tension coefficient depends on the radius of curvature, i.e. $\gamma(R) = \gamma_v(1-4\delta/R)$. For water, Stillinger estimated that δ is approximately equal to 0.5 Å [43]. In the intermediate R range, $2R \geq a$, $W(R)$ can be expanded in powers of R; the first three expansion coefficients are obtained by matching the function and its first two derivatives, given at $R = a$ by Eq. (34). The third derivative is discontinuous at $R = a$ and cannot be obtained in this way. However, from Eq. (35), the R^3 term is likely to be negligible, and in any case, volume and surface area will often be correlated in practice, so that the R^3 term can be included in the surface term. Thus, the expansion effectively has the same form as Eq. (35) to third order, and can be considered an extension of the surface tension concept to molecular dimensions. In practice, the pV-like term is expected to be negligible (atmospheric pressure corresponds to an energy of 1.5×10^{-5} kcal/mol per Å^3) and the free energy is dominated by the surface term. SPT has been compared with results from molecular dynamics simulations and free energy perturbation calculations for non-polar rare gases [49,50].

4.1.2. Solvent-exposed area

SPT provides an important conceptual basis for relating the non-polar free energy contribution to the solvent-exposed surface area. The length scale δ is such that the curvature dependency does not become significant until the radius R is very small (of molecular dimensions). Following this idea, an attractive approximation to Eq. (28) is to ignore curvature effects and write:

$$\Delta W^{(np)}(\mathbf{X}) = \gamma_v A_{tot}(\mathbf{X}) \quad (36)$$

Such a description of the non-polar contribution to the free energy has been extensively used in biophysical applications [51–53].

As first pointed out by Tanford [46], Eq. (36) suggests that there is a close relationship between the macroscopic air–water surface tension, interfacial free energies, and the hydrophobic effect. In practical applications, the surface tension γ_v is usually obtained from experimental data. The limitations of the surface area model are illustrated by vapor-to-water transfer free energies of saturated alkanes in Fig. 1 [53]. Proportionality of the solvation free energy to solute area is good for linear alkanes, but poor for saturated cyclic alkanes. The proportionality coefficient, or 'surface tension', for linear alkanes is approximately 6 cal/mol per Å^2 for vapor-to-water transfer (Fig. 1) and 25 cal/mol per Å^2 for cyclohexane-to-water transfer. The latter value is approximately one-third of the macroscopic water–alkane surface tension (70 cal/mol per Å^2); this observation led Honig et al. to suggest that solvation free energies derived from experimental partition coefficients needed to be corrected to include non-ideal mixing effects, calculated for example by use of Flory–Huggins theory [51,52]. In fact, most experimental data (e.g. Fig. 1) are obtained in ideal-dilute conditions where non-ideal mixing effects are irrelevant [54,55]. The difference between the optimal parameter γ_v for alkanes and the true macroscopic surface tension is simply an effect of the microscopic length scale and the crudeness of the model. For detailed discussions see Holzer [56] and Ben-Naim and Mazo [57].

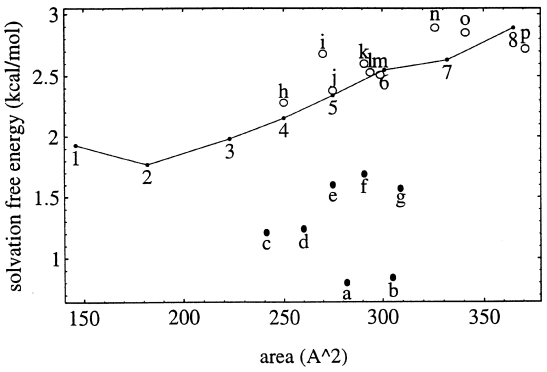

Fig. 1. Vapor-to-water transfer data for saturated hydrocarbons as a function of accessible surface area [133]. Standard states are 1 M ideal gas and solution phases. Linear alkanes (small dots) are labeled by the number of carbons. Cyclic compounds (large dots) are: a = cyclooctane, b = cycloheptane, c = cyclopentane, d = cyclohexane, e = methylcyclopentane, f = methylcyclohexane, g = *cis*-1,2-dimethylcyclohexane. Branched compounds (circles) are: h = isobutane, i = neopentane, j = isopentane, k = neohexane, l = isohexane, m = 3-methylpentane, n = 2,4-dimethylpentane, o = isooctane, p = 2,2,5-tri-methylhexane. Adapted with permission from Simonson and Brünger [53]. Copyright 1994, American Chemical Society.

4.2. Electrostatic contribution

To calculate the electrostatic contribution, $\Delta W^{(\mathrm{elec})}$, one can conveniently choose to scale the atomic partial charges of the solute linearly with the coupling parameter λ_2, i.e.

$$U_{\mathrm{uv}}^{(\mathrm{elec})}(\mathbf{X},\mathbf{Y};\lambda_2) = \sum_{i,j} (\lambda_2 q_{\mathrm{u},i}) q_{\mathrm{v},i} \frac{1}{|\mathbf{x}_i - \mathbf{r}_j|} \qquad (37)$$

where $\mathbf{x}_i$ and $\mathbf{r}_j$ are the position of the ith and jth atom of the solute and the solvent, respectively. Since the solute atom positions $\mathbf{x}_i$ are fixed and only the solvent degrees of freedom $\mathbf{Y}$ are allowed to vary, the electrostatic contribution is, according to Eq. (32),

$$\begin{aligned}
\Delta W^{(\mathrm{elec})}(\mathbf{X}) &= \int_0^1 \mathrm{d}\lambda_2 \left\langle \sum_{i,j} \frac{q_{\mathrm{u},i} q_{\mathrm{v},j}}{|\mathbf{x}_i - \mathbf{r}_j|} \right\rangle_{(\mathbf{X},\lambda_2)} \\
&= \int_0^1 \mathrm{d}\lambda_2 \int \mathrm{d}\mathbf{r} \sum_i \frac{q_{\mathrm{u},i}}{|\mathbf{x}_i - \mathbf{r}|} \\
&\qquad \langle \sum_j q_{\mathrm{v},j} \delta(\mathbf{r} - \mathbf{r}_j) \rangle_{(\mathbf{X},\lambda_2)} \\
&= \int_0^1 \mathrm{d}\lambda_2 \sum_i q_{\mathrm{u},i} \int \mathrm{d}\mathbf{r} \frac{1}{|\mathbf{x}_i - \mathbf{r}|} \\
&\qquad \langle \rho_{\mathrm{elec}}(\mathbf{r}) \rangle_{(\mathbf{X},\lambda_2)} \\
&= \int_0^1 \mathrm{d}\lambda_2 \sum_i q_{\mathrm{u},i} \langle \psi_{rf}(\mathbf{x}_i) \rangle_{(\mathbf{X},\lambda_2)} \qquad (38)
\end{aligned}$$

where $\langle \rho_{\mathrm{elec}}(\mathbf{r})\rangle_{(\mathbf{X},\lambda_2)}$ and $\langle \psi_{rf}(\mathbf{x})\rangle_{(\mathbf{X},\lambda_2)}$ are, respectively, the average solvent charge density and the average solvent reaction field electrostatic potential, for a solute with scaled charges $\lambda_2 q_{\mathrm{u},i}$ in the fixed configuration $\mathbf{X}$ (the subscript $\lambda_1 = 1$ has been omitted for clarity). This equation is exact and provides a formal link to continuum electrostatic approximations (see below).

4.2.1. The Born model

The Born model [58] for the solvation of spherical ions is useful to illustrate the various factors involved in the electrostatic contribution to the free energy. In particular, its microscopic basis has been examined in detail [59–61]. In the Born model, the excess chemical potential is a function of the charge of the ion Q_{ion}, its radius R_{ion}, and the dielectric constant of the solvent ϵ_{v},

$$\Delta W^{(\mathrm{elec})} = \frac{Q_{\mathrm{ion}}^2}{2R_{\mathrm{ion}}}\left(\frac{1}{\epsilon_{\mathrm{v}}} - 1\right). \tag{39}$$

This expression, corresponding to the reversible electrostatic work to charge up an ion in a continuum dielectric solvent, is easily derived using Eq. (38). Typically, the solvent charge density $\langle \rho_{\mathrm{elec}}(\mathbf{r})\rangle$ is sharply peaked at $r = R_{\mathrm{ion}}$, the solute–solvent boundary. This is illustrated in Fig. 2 in the case of two simple ions, K^+ and Cl^-. Neglecting the width of the charge density, the solvent reaction field can thus be approximated as

$$\langle \psi_{\mathrm{rf}}\rangle_{(\lambda_2)} = 4\pi\int_0^\infty r^2 \mathrm{d}r \frac{1}{r}\langle \rho_{\mathrm{elec}}(r)\rangle_{(\lambda_2)}$$

$$\approx \frac{1}{R_{\mathrm{ion}}} 4\pi\int_0^\infty r^2 \mathrm{d}r \langle \rho_{\mathrm{elec}}(r)\rangle_{(\lambda_2)} \tag{40}$$

where the integral on the right-hand side represents the total average solvent charge around the ion. According to Gauss's theorem [63], for a charge $\lambda_2 Q_{\mathrm{ion}}$ in a medium of dielectric constant ϵ_{v}, the total solvent charge density obeys the sum rule [61],

$$4\pi\int_0^\infty r^2 \mathrm{d}r\, \langle \rho_{\mathrm{elec}}(r)\rangle_{(\lambda_2)} = \lambda_2 Q_{\mathrm{ion}}\left(\frac{1}{\epsilon_{\mathrm{v}}} - 1\right) \tag{41}$$

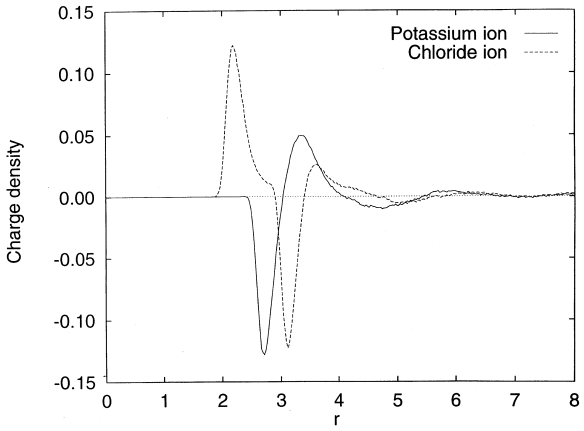

Fig. 2. The solvent charge distribution (in unit charge per Å^3) around K^+ (solid line) and Cl^- (dash line) calculated from molecular dynamics simulations with explicit water molecules is shown. The Lennard–Jones parameters of the ions were adjusted to yield the same solvation free energy as in bulk water, i.e. -80 kcal/mol. For the K^+ (solid line), a first large peak arising from the electronegative water oxygen (at 2.7 Å) is followed by a second smaller peak arising from the electropositive water hydrogens (at 3.5 Å). For the Cl^- (dash line), the structure is different because of the negative charge of the ion. The first peak arising from the water hydrogens (at 2.1 Å) is followed by a second peak arising from the water oxygen (at 3.1 Å and a small and broad peak caused by water hydrogens at 3.9 Å). In the bulk liquid, the integral of the radial charge density surrounding an ion of charge Q is equal to $Q\,(1/\epsilon - 1)$. Adapted with permission from Roux [62].

and the reaction field is (in the continuum limit)

$$\langle \psi_{\mathrm{rf}}\rangle_{(\lambda_2)} \approx \frac{1}{R_{\mathrm{ion}}}\lambda_2 Q_{\mathrm{ion}}\left(\frac{1}{\epsilon_v} - 1\right). \tag{42}$$

Since the solvent reaction field is proportional to the coupling parameter (linear response), the thermodynamic integration over λ_2 yields a factor of one-half in Eq. (39).

As shown by Eq. (40), the magnitude of the free energy is very sensitive to the position of the solute–solvent boundary (i.e. the size of R_{ion} in the case of the Born model). In the continuum limit, it is assumed that the charge density is completely concentrated at the solute–solvent boundary, R_{ion}. In contrast, the solvent charge density in an atomic model is distributed over a microscopic region of finite dimensions as illustrated in Fig. 2. The size of this microscopic

region has important consequences for the reaction field at the center of a spherical cavity, and thus, for the solvation free energy. For this reason, the Born radius must be considered as a state-dependent, empirical parameter that must be adjusted to yield accurate results [61]. In particular, the Born radius is a property of an ion in a given solvent. The Born model of solvation provides the basis for continuum electrostatics approaches for describing the solvation of polar molecular or irregular shapes. These approaches are discussed below.

4.2.2. Classical continuum electrostatics

Continuum electrostatics approximations in which the solvent is represented as a featureless dielectric medium are an increasingly popular approach to describe solvation of polar molecules. Such approximations go back to Born [58], Kirkwood [64] and Onsager [65]. Applications in biophysics have been reviewed recently by several authors [66–68]. The approach is remarkably successful in reproducing the electrostatic contribution to the solvation free energy of small solutes [53,69,70] or amino acids [71], as shown by comparisons to free energy simulations with explicit solvent. Continuum electrostatic approximations are based upon the Poisson equation for macroscopic media [63]

$$\nabla \cdot [\, \epsilon(\mathbf{r}) \nabla \psi(\mathbf{r})] = -4\pi \rho_{\mathrm{u}}(\mathbf{r}) \tag{43}$$

where $\psi(\mathbf{r})$ is the electrostatic potential at a point $\mathbf{r}$, $\rho_{\mathrm{u}}(\mathbf{r})$ represents the fixed charge density of the solute, and $\epsilon(\mathbf{r})$ is the position-dependent dielectric constant.

The Poisson Eq. (43) can be solved numerically by mapping the system onto a discrete grid and using a finite-difference relaxation algorithm [72,73]. Alternatively, a surface boundary element method can be used [74–76]. The numerical problem is made easier by making the approximation that the surrounding solvent has an infinite dielectric constant corresponding to that of a conductor [77,78]. A different approach to incorporate the influence of a polar solvent has been proposed and developed by Warshel and coworkers [79], in which the solvent is modeled by a discrete lattice of dipoles that re-orient under the influence of applied electric fields.

It is generally assumed that the dielectric constant is uniform everywhere except in the vicinity of the solute–solvent boundary. If the dielectric constant inside the solute is assumed to be one, the position-dependent dielectric constant $\epsilon(\mathbf{r})$ can be written $\epsilon(\mathbf{r}) = 1 + \theta(\mathbf{r})\,(\epsilon_{\mathrm{v}} - 1)$, where $\theta(\mathbf{r})$ is an excluded volume function varying sharply from zero inside the solute to one outside (see Beglov and Roux [29] for a demonstration based on integral equations). A dielectric constant of one inside the solute is appropriate as long as the solute degrees of freedom are treated explicitly (for a discussion of *implicit solute* representations, see Section 5.2). To further examine the physical significance of the continuum dielectric approximation, we consider the solvent charge density around the solute [63]

$$\langle\, \rho_{\mathrm{elec}}(\mathbf{r}) \rangle = -\nabla \cdot \mathbf{P}(\mathbf{r}), \tag{44}$$

where $\mathbf{P}(\mathbf{r})$ is the polarization density of the solvent. At any point $\mathbf{r}$ the polarization $\mathbf{P}(\mathbf{r})$ and the total electrostatic field $\mathbf{E}^{\mathrm{tot}}(\mathbf{r})$ are linearly related,

$$\mathbf{P}(\mathbf{r}) = \left(\frac{\epsilon(\mathbf{r}) - 1}{4\pi} \right) \mathbf{E}^{\mathrm{tot}}(\mathbf{r}); \tag{45}$$

this relation is usually taken as the definition of the dielectric constant [63,80]. Since there are no permanent charges in the solvent, the divergence of the polarization density in the solvent is zero except near the dielectric boundary [63], and the solvent charge density is a sharply peaked function localized at the solute–solvent interface. Integrating the solvent charge density along an axis perpendicular to the surface over an infinitesimal range (but broader than the range over which θ varies) and making the width of the boundary go to zero, one recovers the usual expression for the surface charge density $\sigma(\mathbf{r}')$, which is the basis of the boundary element formulation [74–76]. The continuum electrostatic contribution to the PMF can thus be expressed as a surface integral,

$$\Delta W^{(\mathrm{elec})}(\mathbf{X}) = \frac{1}{2} \int_S \mathrm{d}\mathbf{s}' \sum_i q_i \frac{\sigma(\mathbf{r}')}{|\mathbf{x}_i - \mathbf{r}'|} \tag{46}$$

As mentioned, results obtained using the continuum electrostatic approximation depend critically on the location of the dielectric boundary between the solute and the solvent. Hence, there is a need to develop a set of empirical parameters in order to obtain quantitative accuracy in continuum electrostatic calculations. Such parameters are state-dependent. For instance, it is necessary to account for the temperature and pressure dependence of the atomic radii used in Eqs. (15) and (16) to determine the dielectric boundary [61,81] if one wishes to calculate the excess entropy and the partial volume of a solute. It is inconsistent to account only of the state-dependence of the solvent dielectric constant, as is often done (see for example Rashin and Namboodiri [82]). Honig and co-workers have optimized a set of radii based on the experimental free energy of a series of small molecules [70]. We noted above the importance of the average solvent charge distribution function for relating the continuum model to a microscopic description; this relation was exploited recently to derive a different set of optimized atomic radii for peptides and proteins [71].

4.2.3. Treatment of ionic strength

In the presence of mobile ions, the charge density is no longer localized at the solute–solvent interface. Mobile ions are distributed throughout the solvent with number density

$$\rho_i(\mathbf{r};\mathbf{X}) = \bar{\rho}_i \, \mathrm{e}^{-w_i(\mathbf{r};\mathbf{X})/k_\mathrm{B}T}, \tag{47}$$

where i refers to a specific ion type (e.g. counterion or co-ion), $\bar{\rho}_i$ is the number density far from the solute, and $w_i(\mathbf{r};\mathbf{X})$ is the PMF for counterions of type i at position $\mathbf{r}$ for a given solute configuration $\mathbf{X}$ (see also Eq. (23)). The density $\rho_i(\mathbf{r};\mathbf{X})$ contains an excluded volume term, i.e. ion–solute van der Waals interactions prevent ions from penetrating the solute. The ion density can be made to appear explicitly in the Poisson equation, giving the exact form of the Poisson–Boltzmann (PB) equation,

$$\nabla\cdot[\,\epsilon(\mathbf{r})\nabla\psi(\mathbf{r})] = -4\pi\rho_\mathrm{u}(\mathbf{r}) - 4\pi\sum_i q_i\,\bar{\rho}_i\,\mathrm{e}^{-w_i(\mathbf{r};\mathbf{X})/k_\mathrm{B}T}, \tag{48}$$

where the sum is over the different ion types, and $\rho_\mathrm{u}(\mathbf{r})$ indicates the fixed charge density of the solute. The traditional Debye–Hückel treatment [54,83] first approximates the PMF $w_i(\mathbf{r})$ by the electrostatic energy of an ion at $\mathbf{r}$, times the excluded volume function $\theta(\mathbf{r})$:

$$e^{-w_i(\mathbf{r})/k_\mathrm{B}T} \approx \theta(\mathbf{r})e^{-q_i\psi(\mathbf{r})/k_\mathrm{B}T}. \tag{49}$$

Here, $\theta(\mathbf{r})$ is usually assumed to be the same as the function used above to define the dielectric constant $\epsilon(\mathbf{r})$. Eq. (49) is thought to be exact in the limit of very low ion concentrations and far from the solute. Inserting Eq. (49) into Eq. (48) gives what is usually termed the non-linear PB equation. If the exponential in Eq. (48) is linearized one obtains the linearized PB equation [54,67]. This approximation is appropriate at low ion concentrations (where ions are far from the solute and each other on average).

Linearization is a necessary condition for the electrostatic potential to satisfy the fundamental reciprocity relation, $q_a\psi_b = q_b\psi_a$, where q_a and q_b are permanent charges and ψ_b (resp. ψ_a) is the potential produced by at q_b (resp. ψ_a) with q_a (resp. q_b) as the sole source. Without reciprocity, the 'free energy' given by Eq. (49) for a pair of charges becomes dependent on the manner in which the pair is formed (e.g. which one is brought from infinity into the field of the other). More generally, the result of Eq. (49) becomes dependent on the pathway taken to form the system; e.g. different results are obtained by turning on the solute charges while simultaneously allowing the ionic atmosphere to form, and by introducing the ionic atmosphere after the solute charges are turned on. Although this problem has been recognized for many years, its practical importance is still not fully explored. A variational argument has been used to construct a thermodynamic potential applicable with the non-linear PB equation [84].

5. Miscellaneous approximations of implicit solvation

5.1. Solvent boundary potentials and implicit / explicit mixed schemes

A description in which all atomic and structural

details of the solvent molecules are ignored may not always be desirable. In some cases, it may be advantageous to use a mixed scheme which combines an implicit solvent model with a limited number of explicit solvent molecules. For example, one intermediate approach consists in including a small number of explicit solvent molecules in the vicinity of the solute, and representing the remaining bulk with an effective solvent boundary potential [86–92]. The first to design such a simulation method appropriate for liquids were Berkowitz and McCammon [85]. In their method, the many-body system was divided into three main spherical regions: a central reaction region, a buffer region and a surrounding static reservoir region. The forces arising from the reservoir region were calculated from fixed atomic centers. Instead of using explicit fixed atomic centers in the bath region, Brooks and Karplus introduced a mean force field approximation (MFFA) to calculate a soft boundary potential representing the average influence of the reservoir region on the reaction region [86]. In the MFFA treatment, the boundary potential was calculated by integrating all contributions to the average force arising from the reservoir region. The MFFA approach was extended by Brunger et al. for the simulation of bulk water [87]. A similar potential for water droplets of TIP4P was developed by Essex and Jorgensen [88]. The average electrostatic reaction field was taken into account in the surface constrained all-atom solvent (SCAAS) treatment of King and Warshel [90], and in the reaction field with exclusion (RFE) of Rullmann and van Duijnen [91].

Beglov and Roux reformulated the problem of a flexible solvent boundary on the basis of a formal separation of the multidimensional solute–solvent configurational integral in terms of 'inner' solvent molecules nearest to an arbitrary solute, and the remaining 'outer' bulk solvent molecules [92]. In this formulation, it was recognized that the solvent boundary potential corresponds to the solvation free energy of an effective cluster comprising the solute and inner explicit solvent molecules embedded in a large hard sphere. The hard sphere corresponds to a configurational restriction on the outer bulk solvent molecules; its radius is variable, such that it includes the most distant inner solvent molecule. An approximate spherical solvent boundary potential (SSBP) based on this formulation was shown to yield accurate results in computer simulations [92].

The constraint of a spherical shape in most boundary potentials is a limitation. To account for large fluctuations in shape, as in folding–unfolding events, a flexible potential for non-spherical boundaries was developed [93]. This problem is discussed further by Rebecca Wade elsewhere in this volume.

5.2. Implicit solute models

Most of the discussion so far assumed that the solute was in a fixed configuration **X** and that only the degrees of freedom of the solvent were integrated out. In this description, the solute remains fully explicit with all atomic details. Another important class of applications uses implicit solvent models in combination with implicit models of some or all of the solute degrees of freedom; i.e. some or all of the protein degrees of freedom are 'integrated out'. The most important examples are PB treatments of proteins in solution [66,94]. To review these is beyond the scope of this article. Rather, we discuss briefly the relationship between the protein dielectric constant(s) used in PB models and the fluctuations of the protein degrees of freedom that have been integrated out. The simplest process one can consider in a PB treatment of a protein is the insertion of one or a few charges on existing atoms, as in the oxidation of a co-factor. At low ionic strength, in the case of a single perturbing charge q, the charging free energy is [63]

$$\Delta G(0 \rightarrow q) = q\psi_0 + \tfrac{1}{2} q\psi_q, \tag{50}$$

where ψ_0 is the potential at the charge site in the absence of q and ψ_q is the reaction potential induced by q. From the linearity of the PB equation at low ionic strengths, the second term can be calculated with q as the sole source charge, i.e. the second term is equal to the self-energy of q. It is also quadratic with respect to q (since ψ_q is

proportional to q), and from linear response theory it is identical to the relaxation (or 'reorganization') free energy of the system in response to q [95]. The first term has been referred to as the 'static' free energy [95,96].

If the structure of both the reactant (without q) and product (with q) structures are known, the charge insertion can be performed in several equivalent ways, e.g. by inserting fractional charges λq and $(\lambda-1)q$ from either endpoint. Denoting $\Delta G_s^{\mathrm{reac}}$, $\Delta G_r^{\mathrm{reac}}$, $\Delta G_s^{\mathrm{prod}}$, $\Delta G_r^{\mathrm{prod}}$ the static and relaxation free energies to insert a charge $q=1$ at either endpoint, the overall free energy takes the form [96]

$$\Delta G(0\rightarrow q)=\lambda q\Delta G_s^{\mathrm{reac}}+(1-\lambda)q\Delta G_s^{\mathrm{prod}} + \lambda^2 q^2\Delta G_r^{\mathrm{reac}}-(1-\lambda)^2 q^2\Delta G_r^{\mathrm{prod}}. \tag{51}$$

Requiring that the result be independent of λ gives the important relations

$$\Delta G_r^{\mathrm{reac}}=\Delta G_r^{\mathrm{prod}}=\frac{1}{2q}(\Delta G_s^{\mathrm{prod}}-\Delta G_s^{\mathrm{reac}}). \tag{52}$$

These equations follow from the linear response assumption, and are in fact more general than the continuum model. They are known in theories of charge transfer [97]. They connect the change in electrostatic potential going from reactant to product structures (associated with structural relaxation) with the relaxation free energy calculated at either endpoint.

The dielectric constant used to calculate the relaxation free energy is in principle comparable to the Fröhlich–Kirkwood dielectric constant obtained from molecular dynamics simulations [98]. Indeed, the latter is a linear response coefficient describing the polarizability of the solute [80]. Simulations of six proteins were consistent with a low dielectric constant of 2–4 throughout the protein bulk, and a much higher one at the surface where charged groups are located [99–101]. The optimal dielectric constant for relaxation free energy calculations can also be obtained by a test charge approach [95]. The relaxation free energy in response to a small test charge can be estimated from a molecular dynamics simulation of the reactant system using a linear response approximation; many test charge locations can be treated with a single simulation. These free energies can be compared to a Poisson model and the solute dielectric constant adjusted to yield a good fit. Once the relaxation free energies have been calculated, the static free energy can be calculated at both endpoints, and the difference $\Delta G_s^{\mathrm{prod}}-\Delta G_s^{\mathrm{reac}}$ compared to $\Delta G_r^{\mathrm{reac}}$ and $\Delta G_r^{\mathrm{prod}}$ through Eq. (52) [96]. Unlike $\Delta G_r^{\mathrm{reac}}$ and $\Delta G_r^{\mathrm{prod}}$, the static free energy depends (strongly) on the charge set used in the continuum model. Therefore, the optimal dielectric constant for the calculation of the static free energy will depend on the charge set. When a charge set optimized for molecular dynamics in solution is used, it is likely that a dielectric constant of one will be required (for the static term) in order to achieve agreement between the static and relaxation terms [in the sense of Eq. (52)], as observed recently [96]. This leads to a continuum model with two solute dielectric constants: one for the relaxation term and another for the static term, consistent with recent proposals by Krishtalik et al. [100,102]. In more complex processes such as ion or substrate binding, the optimal dielectric constant is not always related in a simple way to the underlying fluctuations of the protein; various operational definitions are then possible [96,103].

5.3. Semi-analytical treatments of continuum electrostatics

In some contexts, even the relatively simple continuum electrostatics approximation based on the exact solution to Eq. (46) may be too expensive computationally. For this reason, approximations to continuum electrostatics based on analytical functions have been developed. The general idea is the following. Since the equations of continuum electrostatics are linear, the free energy $\Delta W^{(\mathrm{elec})}(\mathbf{X})$ can be rigorously expressed as

$$\Delta W^{(\mathrm{elec})}(\mathbf{X})=\frac{1}{2}\int_S \mathrm{d}\mathbf{s}'\sum_{i,j} q_i q_j \frac{\sigma(\mathbf{r}':\mathbf{x}_j)}{|\mathbf{x}_i-\mathbf{r}'|} \tag{53}$$

where $\sigma(\mathbf{r}':\mathbf{x}_j)$ is the surface charge induced at $\mathbf{r}'$ by a unit solute charge located at $\mathbf{x}_j$. Performing the surface integral, this can also be written as

$$\Delta W^{(\mathrm{elec})}(\mathbf{X}) = \frac{1}{2}\sum_{i,j} q_i q_j F(\mathbf{x}_i,\mathbf{x}_j). \tag{54}$$

where $F(\mathbf{x}_i,\mathbf{x}_j)$ is a geometry-dependent coupling function involving all the charges inside the solute. The sum is often separated into two terms,

$$\Delta W^{(\mathrm{elec})}(\mathbf{X}) \frac{1}{2}\sum_{i} q_i^2 F(\mathbf{x}_i,\mathbf{x}_i) + \frac{1}{2}\sum_{i\neq j} q_i q_j F(\mathbf{x}_i,\mathbf{x}_j) \tag{55}$$

where the first term corresponds to a self-interaction, and the second to the charge–charge coupling [analogous to Eq. (50)]. It is noteworthy that the free energy is a superposition of pair-wise additive terms (which depend on the geometry of the solute–solvent dielectric interface). This suggests that it is possible to treat pairs of charges individually. Semi-analytical approaches seek a suitable closed-form approximation for the coupling function $F(\mathbf{x}_i,\mathbf{x}_j)$. Different approximations to $F(\mathbf{x}_i,\mathbf{x}_j)$ have been proposed for complex solutes of irregular shape: the field integrated electrostatic approach (FIESTA) [104], the inducible multipole solvation model (IMS) [105], the analytical continuum electrostatics approach (ACE) [106], and the generalized Born (GB) approach [107].

The strategy is to design an analytical function $F(\mathbf{x}_i,\mathbf{x}_j)$ that yields correct solutions in the limits of large and small charge separation. As an illustration, let us consider the GB approximation for two ions of radius R_1 and R_2 at a distance x_{12} in a continuum solvent [107],

$$\begin{aligned}\Delta W^{(\mathrm{elec-GB})}(\mathbf{x}_1,\mathbf{x}_2) &= \frac{1}{2}\left(\frac{1}{\epsilon_{\mathrm{v}}}-1\right)\left(\sum_{ij}\frac{q_i q_j}{f_{\mathrm{GB}}(x_{ij})}\right)\\ &= \left(\frac{1}{\epsilon_{\mathrm{v}}}-1\right)\left(\frac{1}{2}\sum_i \frac{q_i^2}{R_i}\right.\\ &\quad \left.+\sum_{i<j}\frac{q_i q_j}{f_{\mathrm{GB}}(x_{ij})}\right)\end{aligned} \tag{56}$$

where $f_{\mathrm{GB}}(x_{ij}) = (x_{ij}^2 + R_i R_j \exp[-x_{ij}^2/(4R_iR_j)])^{1/2}$ is the GB function. For superimposed charges q_1 and q_2, the GB function leads to the correct Born solvation free energy for the total charge q_1+q_2, which is obtained as the sum of the GB cross-term and the individual Born solvation free energies of q_1 and q_2. When the pair of charges is slightly separated, i.e. by $x_{ij} < 0.1(R_iR_j)^{1/2}$, the Onsager reaction field is also obtained correctly, within 10%. The Born energy plus a shielded Coulomb charge–charge interaction is obtained when $x_{ij} > 2.5(R_iR_j)^{1/2}$. Because of its simplicity, GB is an effective approach to incorporate solvent effects into semi-empirical ab initio calculations on small molecules [108]. For larger solutes such as a protein, one difficulty is to adjust the radii R_i in order to account for charge burial. Different algorithms have been proposed to solve this problem [106,109].

5.4. Solvent-exposed area models

Solvent-exposed area models assume that the solvation free energy of a solute can be represented as a linear sum of atomic contributions weighted by solvent-exposed area:

$$\Delta W(\mathbf{X}) = \sum_i \gamma_i A_i(\mathbf{X}). \tag{57}$$

Here, A_i is the solvent-exposed area of atom i (which depends on the solute configuration $\mathbf{X}$) and γ_i is an atomic free energy per unit area. This approach leads to free energy models that are essentially geometric [110,111]. Solvent-exposed area models are loosely based on the idea that the solvation free energy arises from a short-range contact between the solute atoms and the solvent. In particular, the non-polar contribution to the free energy arises from a short-range perturbation of the uniform solvent by the solute (see Section 4.1). Likewise, the solvent charge $\sigma(\mathbf{r})$ [as shown in Eq. (46)] is localized near the solute (although the magnitude of the surface

charge actually depends on long-range electrostatic interactions).

Because it is so simple, this approach is widely used in computations on biomolecules [112–114]. Slight variations of the solvent-exposed area models are the shell model of Scheraga [115,116], the excluded-volume model of Colonna and Sander [117,118], and the Gaussian model of Lazaridis and Karplus [119,120] (see also the article by No et al., elsewhere in this volume). Since the calculation of an accurate molecular surface and its analytical derivative with respect to atomic positions can be expensive, Janin and Wodak have proposed and developed an approximate expression for the molecular surface area in macromolecules [121]. This approximate expression has been parameterized for molecular dynamics simulations of proteins [114].

One major problem with implicit solvent-exposed area models is the difficulty in taking into account the dielectric shielding of electrostatic interactions between charged particles. The solvent-exposed area models include the free energy cost of taking a charged residue and burying it in the interior of the protein; this self-interaction energy corresponds to the first term in Eqs. (50) and (55). However, as two charged particles move from the solvent to the non-polar core of the protein, their electrostatic interactions should vary from $q_1 q_2 / \epsilon_v x_{12}$ when they are fully exposed to the solvent, to a very different form when they are fully buried in the protein. Such problems are avoided in semi-analytical treatments of electrostatics (see Section 5.3 above). Elsewhere in this volume, Li et al. describe a solvation model which combines both the GVB reaction field and a careful parametrization of atomic surface tensions.

Lastly, the treatment of protein–solvent and protein–protein interactions must be consistent with the empirical reference state. Experimental free energies of transfer from aqueous solution to weakly polar solvents (e.g. octanol) are often used to model the transfer to the interior of protein. In practical applications, it is difficult to completely avoid a double counting of non-polar protein–protein interactions, since they are present both in the atomic model of the protein and in the empirical free energy scale.

5.5. Knowledge-based potentials

One of the greatest problems in predicting the three-dimensional fold of a protein is the need to search over a large number of possible configurations to find the global free energy minimum. For extensive configurational searches, it is necessary to use a free energy function $W(\mathbf{X})$ that is as simple and inexpensive as possible. Knowledge-based potentials are the simplest such free energy functions. Such potentials have been constructed empirically from statistical analyses of known protein structures taken from structural data bases [122]. The general idea is that the number of residue pairs at a certain distance observed in the data base follows the statistics of a thermal ensemble, in other words a Boltzmann principle [123]. Equivalently, it is assumed that the observed probability of finding a pair of residues at a distance R in a protein structure is related to the Boltzmann factor of an effective distance-dependent free energy. The simplest potentials distinguish only two types of residues: non-polar and polar [122]. No attempts are made to establish a specific relation to the laws of physics. Often, the knowledge-based potentials do not resemble the microscopic interactions that would be expected between residues in an atomic description. For example, one of the simplest potentials, designed by Sippl [122], is attractive for pairs of non-polar residues and repulsive for pairs of polar residues. Nevertheless, the resulting structures that are obtained via conformational searches, usually with an additional restraint on the protein radius of gyration, are reasonable: the non-polar residues tend to form a hydrophobic core in the center of the structure, while the polar residues tend to be located at the protein surface. There are a growing number of potentials constructed from similar ideas [124–128]. Recently, Mirny and Shakhnovich have re-examined the methods for deriving knowledge-based potentials for protein folding [129]. Their potential is obtained by a global optimization procedure that simultaneously max-

imizes thermodynamic stability for all proteins in the database. This field is in rapid expansion, and it is beyond the scope of the present review to cover all possible developments. For more information, see the reviews [130–132] and references therein.

6. Summary

The microscopic significance of an implicit solvent potential for a solute in a fixed configuration has been clarified. A statistical mechanical formulation of the 'potential of mean force' or 'solvent free energy surface' provides a robust theoretical framework to express the influence of solvent rigorously. Nonetheless, going beyond such formal considerations, it is clear that any implicit model is an approximation that must be parameterized carefully to yield accurate results. Not surprisingly, *there is no free lunch*, and inexpensive approaches are inevitably based on simple ideas that are of unknown validity in untested situations. Thus, implicit solvent models are the result of a compromise which must be constantly analyzed and judged in comparison with experimental results and also more rigorous treatments of solvation (e.g. simulation with explicit solvent molecules).

The decomposition of the free energy in terms of non-polar and electrostatic contributions, as described by Eq. (27), is central to many theoretical approximations. An attractive and commonly used treatment is to write $\Delta W = \Delta W^{(\mathrm{np})} + \Delta W^{(\mathrm{elec})}$, where $\Delta W^{(\mathrm{np})}$ is modeled by a solvent-exposed area term with Eq. (36), while $\Delta W^{(\mathrm{elec})}$ is modeled by a continuum electrostatic reaction field, Eq. (46). Although such a treatment is clearly an approximation, it relies on a reasonable physical picture of solvation. A relationship with first principles and statistical mechanics can be established, and the approximation can be compared with the results of computer simulations with explicit solvent [49,50,69–71]. Recently, Vorobjev and Hermans have used such an implicit solvent model to successfully discriminate models from a data base of misfolded protein structures [6] (see also the article in this volume).

In some cases it is necessary to use treatments that are even less expensive computationally than the PB equation. Several semi-analytical approximate treatments of the continuum electrostatic problem have been proposed (e.g. GB [107], FIESTA [104], ACE [106] and IMS [105]). A careful parameterization of such a model can yield remarkably accurate results for a number of small to medium-size molecules (see the article by Li et al. in this volume). Even these approximations may appear too expensive for the extensive conformational searches that are required to address the protein folding problem. In that case, empirical constructs and information-based potentials are used to mimic and reproduce the statistical trends observed in macromolecular structures. The microscopic basis of these last approaches is not yet formally linked to a statistical mechanical formulation of implicit solvent.

Acknowledgements

Financial support from FCAR (Québec) and CNRS (France) is acknowledged. B.R. is a research fellow of the Medical Research Council of Canada.

References

[1] C.L. Brooks III, M. Karplus, B.M. Pettitt, Proteins a theoretical perspective of dynamics, structure and thermodynamics, in: I. Prigogine, S.A. Rice (Eds.), Advances in Chemical Physics, vol. LXXI, John Wiley and Sons, New York, 1988.
[2] M.P. Allen, D.J. Tildesley, Computer Simulation of Liquids. Oxford Science Publications, Clarendon Press, Oxford, 1989.
[3] D.A. McQuarrie, Statistical Mechanics, Harper and Row, New York, 1976.
[4] J.G. Kirkwood, J. Chem. Phys. 3 (1935) 300.
[5] R.W. Zwanzig, J. Chem. Phys. 22 (1954) 1420–1426.
[6] Y.N. Vorobjev, J.C. Almagro, J. Hermans, PROT. Struc. Funct. Gen. 32 (1998) 399–413.
[7] M.K. Gilson, J.A. Given, B.L. Bush, J.A. McCammon, Biophys. J. 72 (1997) 1047–1069.
[8] P. Smith, B.M. Pettitt, M. Karplus, J. Phys. Chems. 97 (1993) 6907–6913.
[9] R. Zwanzig, J. Stat. Phys. 9(3) (1973) 215–220.
[10] S.A. Adelman, Adv. Chem. Phys. 44 (1980) 143–251; S.A. Adelman, J. Chem. Phys. 73 (1980) 3145–3158.
[11] R. Kubo, Rep. Prog. Phys. 29 (1966) 255–284.
[12] H.J.C. Berendsen, W.F. van Gunsteren, J.A.C. Rullmann, Faraday Disc. Chem. Soc. 66 (1978) 58–70.

[13] J.P. Hansen, I.R. McDonald, Theory of Simple Liquids, Academic Press, London, 1976.
[14] D. Chandler, The equilibrium theory of polyatomic fluids, in: E.W. Montroll, J.L. Lebowitz (Eds.), The Liquid State of Matter: Fluids, Simple and Complex, vol. VIII, North-Holland, Amsterdam, 1982.
[15] P.H. Fries, G.N. Patey, J. Chem. Phys. 82 (1985) 429–440.
[16] D. Chandler, H.C. Andersen, J. Chem. Phys. 57 (1972) 1930–1937.
[17] F. Hirata, P.J. Rossky, Chem. Phys. Lett. 83 (1981) 329–334.
[18] B.M. Pettitt, P.J. Rossky, J. Chem. Phys. 84 (1986) 5836–5844.
[19] H.A. Yu, M. Karplus, J. Chem. Phys. 89 (1988) 2366.
[20] M.B. Pettitt, M. Karplus, Chem. Phys. Lett. 136 (1987) 383–386.
[21] W.F. Lau, B.M. Pettitt, Biopolymers 26 (1987) 1817–1831.
[22] G. Ramé, W.F. Lau, B.M. Pettitt, Int. J. Pept. Protein Res. 35 (1990) 315–327.
[23] D.A. Zichi, P.J. Rossky, J. Chem. Phys. 84 (1986) 1712–1723.
[24] P.H. Lee, G.M. Maggiora, J. Phys. Chem. 97 (1983) 10175–10185.
[25] L.W. Pratt, D. Chandler, J. Chem. Phys. 67 (1977) 3683.
[26] J.S. Perkyns, B.M. Pettitt, Chem. Phys. Lett. 190 (1992) 626–630.
[27] D. Beglov, B. Roux, J. Chem. Phys. 103 (1993) 360–364.
[28] M. Ikeguchi, J. Doi, J. Chem. Phys. 103 (1995) 5011–5017.
[29] D. Beglov, B. Roux, J. Chem. Phys. 104 (1996) 8678–8689.
[30] D. Beglov, B. Roux, J. Phys. Chem. 101 (1997) 7821–7826.
[31] C.M. Cortis, P.J. Rossky, R.A. Friesner, J. Chem. Phys. 107 (1997) 6400–6414.
[32] Y. Liu, T. Ichiye, Chem. Phys. Lett. 231 (1994) 380–386.
[33] J-K Hyun, C.S. Babu, T. Ichiye, J. Chem. Phys. 99 (1995) 5187–15185.
[34] G. Hummer, D.M. Soumpasis, Phys. Rev. E 50 (1994) 5085–5095.
[35] A.E. García, G. Hummer, D.M. Soumpasis, Prot. Struc. Funct. & Gen. 27 (1997) 471–480.
[36] W.D. Cornell, P. Cieplak, C.I. Bayly, et al., J. Am. Chem. Soc. 117 (1995) 5179–5197.
[37] A.D. MacKerell, Jr., D. Bashford, M. Bellot, et al., J. Phys. Chem. B 102 (1998) 3586–3616.
[38] W.L. Jorgensen, D.S. Maxwell, J. Tirado-Rives, J. Am. Chem. Soc. 118 (1996) 11225–11236.
[39] X. Kong, C.L. Brooks III, J. Chem. Phys. 105 (1996) 2414–2423.
[40] T. Simonson, A.T. Brünger, Biochemistry 31 (1992) 8661–8674.
[41] S. Boresch, G. Archontis, M. Karplus, Proteins 20 (1994) 25.
[42] H. Reiss, H.L. Frisch, J.L. Lebowitz, J. Chem. Phys. 31 (1959) 369–380; H. Reiss, Adv. Chem. Phys. 9 (1965) 1–84.
[43] F. Stillinger, J. Solution Chem. 2 (1973) 141–158.
[44] R.A. Pierotti, Chem. Rev. 76 (1976) 717–726.
[45] R.C. Tolman, J. Chem. Phys. 16 (1948) 758–774.
[46] C. Tanford, Proc. Natl. Acad. Sci. USA 76 (1979) 4175–4176.
[47] G. Hummer, S. Garde, A.E. Garcia, A. Pohorille, L.R. Pratt, Proc. Nat. Acad. Sci. USA. 93 (1994) 8951.
[48] G. Hummer, S. Garde, Phys. Rev. Lett. 80 (1997) 4193–4196.
[49] J.P. Postma, H.C. Berendsen, J.R. Haak, Faraday Symp. Chem. Soc. 17 (1982) 55.
[50] T.P. Straatsma, H.J.C. Berendsen, J.P.M. Postma, J. Chem. Phys. 85 (1986) 6720.
[51] K. Sharp, A. Nicholls, R. Fine, B. Honig, Science 252 (1991) 106–109.
[52] K. Sharp, A. Nicholls, R. Friedman, B. Honig, Biochemistry 30 (1991) 9696–9697.
[53] T. Simonson, A.T. Brünger, J. Phys. Chem. 98 (1994) 4683–4694.
[54] R.H. Fowler, E.A. Guggenheim, Statistical Thermodynamics, Cambridge University Press, 1939.
[55] A. Ben Naim, J. Phys. Chem. 82 (1973) 792–803.
[56] A. Holzer, Biopolymers 32 (1992) 711–715.
[57] A. Ben-Naim, R. Mazo, J. Phys. Chem. 97 (1993) 10829–10834.
[58] M. Born, Z. Phys. 1 (1920) 45.
[59] A.A. Rashin, B. Honig, J. Phys. Chem. 89 (1985) 5588.
[60] F. Hirata, P. Redfern, R.M. Levy, Int. J. Quantum Chem. 15 (1988) 179.
[61] B. Roux, H.-A. Yu, M. Karplus, J. Phys. Chem. 94 (1990) 4683–4688.
[62] B. Roux, Biophys. J. 71 (1996) 3177–3185.
[63] J.D. Jackson, Classical Electrodynamics, John Wiley and Sons, New York, 1962.
[64] J.G. Kirkwood, J. Chem. Phys. 2 (1934) 351.
[65] L. Onsager, J. Am. Chem. Soc. 58 (1936) 1468–1493.
[66] B. Honig, A. Nicholls, Science 268 (1995) 1144.
[67] K.A. Sharp, B. Honig, Annu. Rev. Biophys. Biophys. Chem. 19 (1990) 301–332.
[68] M.K. Gilson, B. Honig, Protein 4 (1988) 7–18.
[69] A. Jean-Charles, A. Nicholls, K. Sharp, et al., J. Am. Chem. Soc. 113 (1991) 1454–1455.
[70] D. Sitkoff, K.A. Sharp, B. Honig, J. Phys. Chem. 98 (1994) 1978.
[71] M. Nina, D. Beglov, B. Roux, J. Phys. Chem. 101 (1997) 5239–5248.
[72] J. Warwicker, H.C. Watson, J. Mol. Biol. 157 (1982) 671.
[73] I. Klapper, R. Hagstrom, R. Fine, K. Sharp, B. Honig, Proteins 1 (1986) 47.
[74] R. Zauhar, R. Morgan, J. Mol. Biol. 186 (1985) 815–820.
[75] P. Shaw, Phys. Rev. A 32 (1985) 2476–2487.
[76] Y.N. Vorobjev, H.A. Scheraga, J. Comp. Chem. 18 (1997) 569–583.

[77] A. Klamt, G. Schüürmann, J. Chem. Soc. Perkin Trans. 2 (1993) 799.
[78] D.M. York, T.S. Lee, W. Yang, J. Am. Chem. Soc. 118 (1996) 10940–10941.
[79] A. Warshel, J. Åqvist, Annu. Rev. Biophys. Biophys. Chem. 20 (1991) 267–298.
[80] H. Fröhlich, Theory of Dielectrics, Clarendon Press, Oxford, 1949.
[81] E. Whalley, J. Chem. Phys. 38 (1963) 1400–1405.
[82] A.A. Rashin, K. Namboodiri, J. Phys. Chem. 91 (1987) 6003.
[83] P. Debye, E. Hückel, Phys. Z. 24 (1923) 305–325.
[84] K. Sharp, B. Honig, J. Phys. Chem. 94 (1990) 7684–7692.
[85] M. Berkowitz, J.A. McCammon, Chem. Phys. Lett. 90 (1982) 215.
[86] C.L. Brooks III, M. Karplus, J. Chem. Phys. 79 (1983) 6312–6325.
[87] A. Brunger, C.L. Brooks III, M. Karplus, Chem. Phys. Lett. 105 (1984) 495–500.
[88] J.W. Essex, W.L. Jorgensen, J. Comp. Chem. 16 (1995) 951–972.
[89] A. Warshel, G. King, Chem. Phys. Lett. 121 (1985) 124.
[90] G. King, A. Warshel, J. Chem. Phys. 91 (1989) 3647.
[91] J.A. Rullmann, P.Th. van Duijnen, Mol. Phys. 61 (1987) 293.
[92] D. Beglov, B. Roux, J. Chem. Phys. 100 (1994) 9050–9063.
[93] D. Beglov, B. Roux, Biopolymers 35 (1995) 171–178.
[94] N. Rogers, Prog. Biophy. Mol. Biol. 48 (1986) 37–66.
[95] T. Simonson, D. Perahia, J. Am. Chem. Soc. 117 (1995) 7987–8000.
[96] T. Simonson, G. Archontis, M. Karplus, J. Am. Chem. Soc., submitted, 1999.
[97] R. Marcus, Annu. Rev. Phys. Chem. 15 (1964) 155.
[98] M. Gilson, B. Honig, Biopolymers 25 (1986) 2097–2119.
[99] T. Simonson, D. Perahia, Proc. Natl. Acad. Sci. USA 92 (1995) 1082–1086.
[100] T. Simonson, C.L. Brooks, J. Am. Chem. Soc. 118 (1996) 8452–8458.
[101] T. Simonson, J. Am. Chem. Soc. 120 (1998) 4875–4876.
[102] L. Krishtalik, A.M. Kuznetsov, E.L. Mertz, Proteins 28 (1997) 174–182.
[103] Y.Y. Sham, I. Muegge, A. Warshel, Biophys. J. 74 (1998) 1744–1753.
[104] H. Sklenar, F. Eisenhaber, M. Poncin, R. Lavery, in: D.L. Beveridge, R. Lavery (Eds.), Theoretical Biochemistry and Molecular Biophysics, Adenine Press, 1990.
[105] M.E. Davis, J. Chem. Phys. 100 (1994) 5149–5159.
[106] M. Schaefer, M. Karplus, J. Phys. Chem. 100 (1996) 1578–1599.
[107] W.C. Still, A. Tempczyk, R.C. Hawley, T. Hendrickson, J. Am. Chem. Soc. 112 (1990) 6127–6129.
[108] C.J. Cramer, D.G. Truhlar, in: K.B. Lipkowitz (Ed.), Reviews in Computational Chemistry, VCH, New York, 1995.
[109] S.R. Edinger, C. Cortis, P.S. Shenkin, R.A. Friesner, J. Phys. Chem. B101 (1997) 1190.
[110] M.L. Connolly, Science 221 (1983) 709–713.
[111] R.J. Richmond, J. Mol. Biol. 178 (1984) 63–89.
[112] D. Eisenberg, A. McClachlan, Nature 319 (1986) 199–203.
[113] L. Wesson, D. Eisenberg, Protein Sci. 1 (1993) 227–235.
[114] F. Fraternali, W.F. Van Gunsteren, J. Mol. Biol. 256 (1996) 939–948.
[115] H.A. Scheraga, Acc. Chem. Res. 12 (1979) 7–14.
[116] Y.K. Kang, K.D. Gibson, G. Nemethy, H. Scheraga, J. Phys. Chem. 92 (1988) 4739–4742.
[117] F. Colonna-Cesari, C. Sander, Biophys. J. 57 (1990) 1103–1107.
[118] P. Stouten, C. Frömmel, H. Nakamura, C. Sander, Mol. Sim. 10 (1993) 97–120.
[119] T. Lazaridis, M. Karplus, Science 278 (1997) 1928–1931.
[120] T. Lazaridis, M. Karplus, Proteins, submitted, 1998.
[121] S.J. Wodak, J. Janin, Proc. Natl. Acad. Sci. USA 77 (1980) 1736–1740.
[122] M.J. Sippl, J. Mol. Biol. 213 (1990) 859–883.
[123] M.J. Sippl, J. Comput.-Aided Mol. Des. 7 (1993) 473–501.
[124] K. Yue, K.A. Dill, Protein Sci. 5 (1996) 254–261.
[125] I. Bahar, R.L. Jernigan, J. Mol. Biol. 266 (1997) 195–214.
[126] S.H. Bryant, C.E. Lawrence, Proteins 16 (1993) 92–112.
[127] S.E. DeBolt, J. Skolnick, Protein Eng. 9 (1996) 637–655.
[128] K.K. Koretke, Z. Luthey-Schulten, P.G. Wolynes, Protein Sci. 5 (1996) 1043–1059.
[129] L.A. Mirny, E.I. Shakhnovich, J. Mol. Biol. 264 (1996) 1164–1179.
[130] S. Vajda, M. Sippl, J. Novotny, Curr. Opin. Struct. Biol. 7 (1997) 222–228.
[131] D.T. Jones, J.M. Thornton, Curr. Opin. Struct. Biol. 6 (1996) 210–216.
[132] R.L. Jernigan, I. Bahar, Curr. Opin. Struct. Biol. 6 (1996) 195–209.
[133] A. Ben Naim, Y. Marcus, Solvation thermodynamics of nonionic solutes. J. Chem. Phys. 81 (1984) 2016–2027.